2010 IREP Symposium- Bulk Power System Dynamics and Control – VIII (IREP), August 1-6, 2010, Buzios, RJ, Brazil

Effects of Variable Solar Irradiance on the Reactive Power Compensation for Large Solar Farm

Dustin F. Howard, Ronald G. Harley, Jiaqi Liang
School of Electrical and Computer Engineering
Georgia Institute of Technology
Atlanta, GA, USA

Ganesh K. Venayagamoorthy
Real-Time Power and Intelligient Systems Laboratory
Missouri University of Science and Technology
Rolla, MO, USA

Abstract

Dish-Stirling systems are a form of concentrating solar power (CSP) emerging as an efficient and reliable source of renewable energy. Various technical hurdles are involved in the grid interconnection of dish-Stirling systems, particularly with issues related to power factor correction, low voltage ride-through capability, and reactive power planning. While there are no grid-interconnection requirements specific to dish-Stirling technology, the requirements currently established for wind farms are used as a starting point due to the similar design and operating characteristics between wind farms and dish-Stirling solar farms. A dish-Stirling solar farm requires external reactive power compensation to meet the power factor requirements presently set for wind farms. The following paper provides a brief overview of dish-Stirling technology, along with an analysis of methods for meeting power factor grid interconnection requirements and maintaining necessary voltage levels under varying irradiance conditions due to cloud cover. Simulation results for voltage and power factor of the solar farm are provided for both steady state and cloud transient conditions within a 12-bus network.

Introduction

Dish-Stirling technology is a form of concentrating solar power (CSP) which utilizes the thermal energy from solar irradiance to generate electric power. Demonstration units have reached operational success, achieving the world's highest sun-to-grid energy conversion efficiency [1]. The first large-scale solar farm using dish-Stirling technology, rated at 1.5 MW, came online in January 2010 in Peoria, AZ, and installations rated for several hundred megawatts are in the planning stages [2]. As dish-Stirling solar farms increase in capacity, grid interconnection issues become increasingly important, particularly regarding power factor correction and grid fault-ride-through capability [3]. Increasing penetration of dish-Stirling solar farms within the utility grid requires simulation studies to assess the dish-Stirling system's impact on steady state and transient behavior of the grid, a topic which has received scant attention in the literature to date.

A brief overview of dish-Stirling operating principles and control systems is presented, along with analysis and simulation results for a single machine infinite bus (SMIB) model and a solar farm integrated into a 12-bus network. All simulations are run with a complete dish-Stirling model, including the Stirling engine internal working gas dynamics. Different options of reactive power compensation to meet grid interconnection requirements are discussed, and simulation results provided.

System Overview

A diagram of a dish-Stirling system is shown in Fig. 1. The main components of the system are the concentrator, receiver, and power conversion unit (PCU), which contains the Stirling engine, generator, and various system controls. The concentrator is a parabolic dish of mirrors which tracks the sun on two axes and focuses the direct normal insolation (DNI) onto the receiver, which acts as a thermal interface between the concentrated sunlight and the Stirling engine. At the base of the receiver lies the absorber, which is the heat exchanger connected to the Stirling engine. Critical to the receiver operation is the temperature of the absorber. This temperature should be maintained as high as possible to maximize the efficiency of the Stirling engine, but should not exceed the thermal limits of the receiver and absorber materials. Controlling the absorber temperature is the primary task of internal PCU control systems, and can be accomplished by increasing or decreasing the rate of heat transfer to the Stirling Engine. The Stirling engine absorbs heat from the receiver to generate torque to turn the generator shaft. Squirrel cage induction machines are used in most dish-Stirling system designs to-date [4]. The disadvantages of

This work was supported in part by the National Science Foundation, USA, under Grants EFRI #0836017 and ECCS #0802047.

978-1-4244-7467-7/10/$26.00 ©2010 IEEE

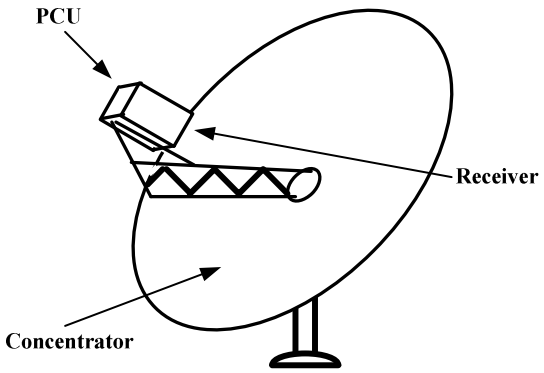

Fig. 1. Dish-Stirling system with labeled components.

using an induction machine are the lack of voltage and frequency control, but with the advantage of low cost and rugged design. Electric cables run from the generator through underground ducts to the utility point of common coupling (PCC). The system returns to a stow-away position in the evening when the sun goes down, and begins operation again the following morning. The ratings of various dish-Stirling systems developed to-date are between 8 and 25 kW per dish at an irradiance of 1000 W/m^2 [4]. Dish-Stirling solar farms consist of hundreds or thousands of individual dish-Stirling units operating in parallel.

Stirling Engine

A diagram of the modeled Stirling engine appears in Fig. 2. The Stirling engine is a closed-cycle external heat engine. A working gas, usually hydrogen or helium, is contained within the engine. The engine contains three heat exchanger volumes, known as the heater, regenerator, and cooler, and two working space volumes, known as the expansion and compression spaces. The heater (or absorber) is directly exposed to the concentrated sunlight. Since the working space volumes are directly coupled to the crankshaft, the volumes vary periodically during operation, causing the working gas to flow between the working spaces, absorbing heat in the heater and expanding in the expansion space. The regenerator is designed to absorb the heat in the working gas as it passes from the heater to the cooler, where it will otherwise be ejected to the atmosphere. When the gas passes back from the cooler to the heater, the regenerator will then return the stored thermal energy to the working gas, thus significantly improving the efficiency of the engine. The torque produced by the Stirling engine is a result of the working gas pressure acting on the pistons.

The modeled Stirling engine is a four cylinder engine containing four sets of heat exchangers. The pistons oscillate with a 90^o phase shift, where each "quadrant" of the engine equally contributes to the torque produced. A more detailed analysis of the modeling of dish-Stirling mechanical, thermal, and working gas dynamics is given in [5].

Control Systems

The absorber temperature is the primary parameter to be controlled in dish-Stirling systems. The efficiency of the Stirling engine increases with absorber temperature, but is limited by the thermal ratings of the absorber and receiver materials. Therefore, the control systems attempt to maintain the highest safe operating temperature, which is achieved by varying the working gas pressure, effectively changing the heat exchange rate between the Stirling engine and the absorber. In addition to controlling the absorber temperature, the engine/generator shaft speed must be controlled, but only during grid-fault transients. In steady state, the speed varies with irradiance, but stays within a narrow range just above synchronous frequency. The torque generated by the Stirling engine does not approach the induction generators pull-out torque rating, thus strict speed control is unnecessary in steady state. However, a grid-fault induces a sharp speed increase of the generator shaft, which can potentially damage system components and prevent the system from recovering from the fault [6]. Both the receiver temperature and the transient over-speed can be controlled by varying the working gas pressure. The pressure control system (PCS) can supply or remove working gas from the Stirling engine's external gas storage tanks. Adding working gas to the engine increases the pressure, which in turn increases the heat exchange rate in the absorber/heater, and vice-versa for decreasing the pressure. In addition, the torque produced by the engine is a function of the working gas pressure, where a decrease in the pressure

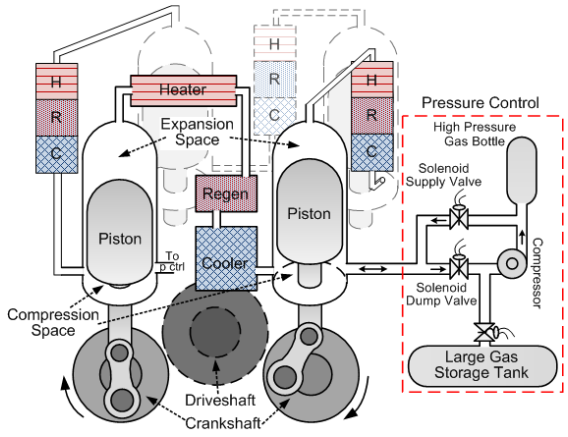

Fig. 2. Physical diagram of the modeled Stirling engine, including the pressure control system with its interconnection with the engine.

causes a decrease in torque. Thus, the over-speed condition induced by a grid fault can be mitigated by quickly decreasing the working gas pressure.

Grid Interconnection Requirements (GIR)

While there are presently no solar farm-specific GIR, it is reasonable to assume that the present requirements for wind farms [7] will be similar if not identical to requirements of dish-Stirling solar farms. The operating characteristics of wind farms and dish-Stirling solar farms are quite similar, particularly due to the intermittent nature of the energy source and the use of induction (asynchronous) generators in many wind turbine designs, which are also used in dish-Stirling systems. Many of the potential dish-Stirling GIR are discussed in [3], while this paper focuses on the following requirements, that a solar farm should be capable of:

- Operating at a power factor anywhere in the range from 0.95 lagging to 0.95 leading at the PCC
- Maintaining a voltage at the PCC between 0.95 and 1.05 pu

Meeting these requirements with dish-Stirling solar farms requires additional infrastructure, since induction machines normally operate at a power factor outside of the range 0.95 lagging to 0.95 leading. In addition, induction machines absorb reactive power when operated as both a motor and a generator, which tends to reduce the voltage at the PCC. The amount of reactive power absorbed depends on the instantaneous solar irradiance, since the torque generated by the Stirling engine varies with input solar thermal energy. In addition, variations in solar irradiance, or cloud cover, cause variations in the voltage at the PCC, since the real power delivered and the reactive power absorbed by the solar farm fluctuates. Since there is no built-in means of voltage control with an induction machine, reactive power compensation is required to both increase the PCC voltage and mitigate the voltage variations due to cloud cover. Reactive power compensation is also required to bring the power factor within an acceptable range. The above requirements can

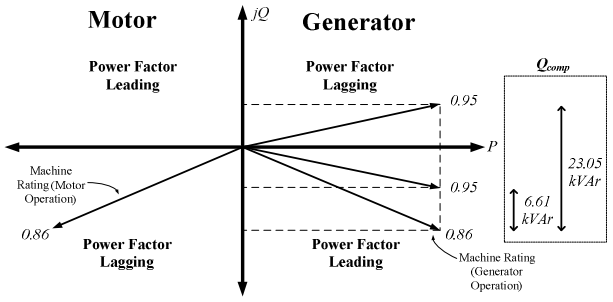

Fig. 3. P-Q diagram of induction machine, showing amount of reactive power compensation required to meet grid interconnection requirements.

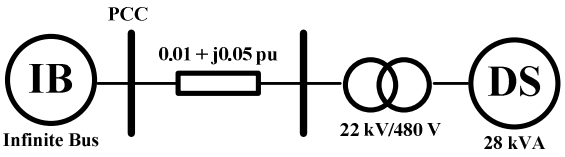

Fig. 4. Connection of a single dish-Stirling (DS) unit in a single machine infinite bus model.

be satisfied with various sources of reactive power compensation, such as switched capacitors or static var compensators (SVCs).

Single Machine Infinite Bus (SMIB) Model

Before proceeding further, a notational clarification is established regarding power factor notation. The positive direction of the generator current, real power, and reactive power is specified as coming out of the generator terminals into the network. With this notational convention, the machine generates power with a leading power factor (with no compensation), similar to the operation of an under-excited synchronous generator. The induction machine absorbs reactive power when operated as both a motor and a generator. However, the power factor changes from lagging to leading when changing from motoring to generating operation, respectively.

The P-Q phasor diagram of Fig. 3 illustrates the amount of compensation required to meet power factor GIR for a single 25 kW dish-Stirling unit. Also shown in Fig. 3 is the power factor notation used for the four operating regions of the induction machine. Reactive power compensation requirements of dish-Stirling solar farms can be calculated assuming rated voltage is applied to the generator terminals, where the rated power factor of the induction machine is assumed. Thus, with a dish-Stirling unit supplying rated power output of 25 kW and with a machine rated power factor of 0.86 leading, the reactive power absorbed, assuming no reactive power compensation, is given by

$$\begin{aligned} Q &= -|V||I|\sin\theta = -P\tan\theta \\ &= -\frac{25}{0.86}\sin\left(\cos^{-1}(0.86)\right) = -14.83 \ \ kVAr \end{aligned} \tag{1}$$

where θ is the angle between the current and voltage waveforms. The reactive power required to supply rated real power at a power factor from 0.95 leading to 0.95 lagging is calculated by

$$\begin{aligned} 0.95 \ \ leading \rightarrow Q_{comp} &= 14.83 - \frac{25}{0.95}\sin\left(\cos^{-1}(0.95)\right) \\ &= 6.61 \ \ kVAr \\ 0.95 \ \ lagging \rightarrow Q_{comp} &= 14.83 + \frac{25}{0.95}\sin\left(\cos^{-1}(0.95)\right) \\ &= 23.05 \ \ kVAr \end{aligned} \tag{2}$$

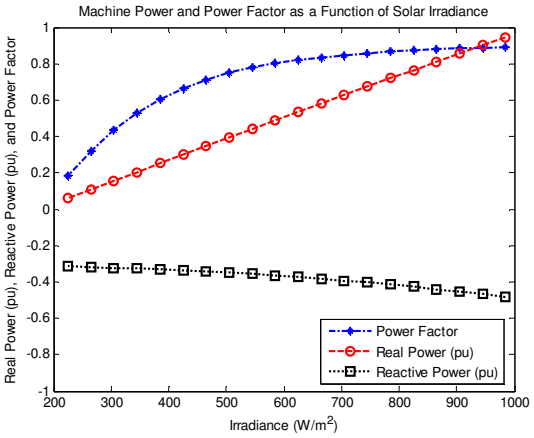

(a)

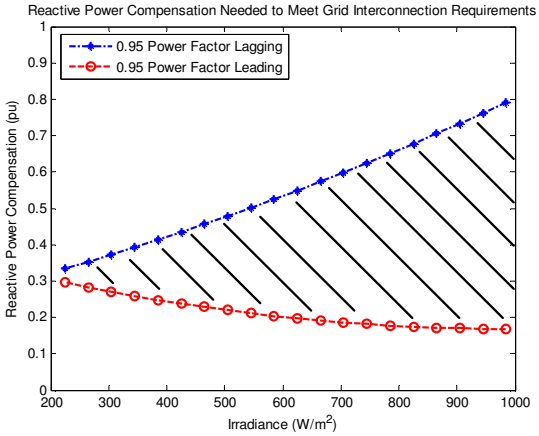

(b)

Fig. 5. (a)Various induction generator parameters as a function of irradiance and (b) reactive power compensation required to meet grid interconnection power factor standard.

Thus the variable reactive power compensation must have a capacity of at least 6.61 kVAr to meet the GIR.

A single dish-Stirling system is connected as shown in Fig. 4. Shown in Fig. 5(a) is the real power, reactive power, and power factor of the induction generator as a function of solar irradiance level. The range of irradiance is chosen to be between 200 and 1000 W/m^2 since this range is typical for most locations around the world, and the dish-Stirling system cannot generally operate at irradiance levels lower than 200 W/m^2 [8]. As expected, the real and reactive power magnitudes increase with irradiance and the power factor improves. The real and reactive power magnitudes decrease roughly linearly with irradiance, but the power factor decreases much more rapidly. Shown in Fig. 5(b) is the reactive power compensation required as a function of irradiance for meeting both the 0.95 leading requirement and 0.95 lagging requirement. The shaded region illustrates that the range of compensation required to operate throughout the entire 0.95 leading to 0.95 lagging region. Therefore, since cloud cover will cause the irradiance to vary during the day, the reactive power compensation should minimally be capable of operating along the lower line of Fig. 5(b). For the case of switched capacitors, discrete quantities of reactive power compensation are available, thus choosing the proper values of capacitors allows for operation at discrete points within the shaded region shown in Fig. 5(b). Continuously variable reactive power compensation, such as SVCs, can operate at any point within the shaded region if properly sized.

While the SMIB model provides a clear conception of the reactive power compensation required to meet GIR, the assumption of an infinite bus is highly idealistic. In addition to the reactive power compensation required to maintain the power factor range, the compensation should also maintain the voltage within an acceptable region. Simulation within a more realistic system is therefore necessary to assess the effects of varying irradiance levels on both voltage and power factor.

12-Bus Network

The 12-bus network used in this analysis and simulation of a dish-Stirling solar farm is shown in Fig. 6. The base-case network consists of 4 generators: three synchronous machines (G2, G3, & G4) and an infinite bus (G1). The various loads are modeled with passive components and the interconnecting lines are modeled using pi-equivalent models. The synchronous machines' excitation systems are included in the modeled network, along with the turbine governors and automatic voltage regulators (AVRs). More details of the 12-bus network are given in [9].

For simulation of the solar farm within the 12-bus network, the individual solar farm generators are lumped into a single induction machine model with the same MW rating of the sum total of all the individual induction machines. Different scenarios for incorporating a solar farm into the 12-bus network at bus 11, with the PCC at bus 3, are analyzed in order to assess the impact of incorporating the solar farm into the network

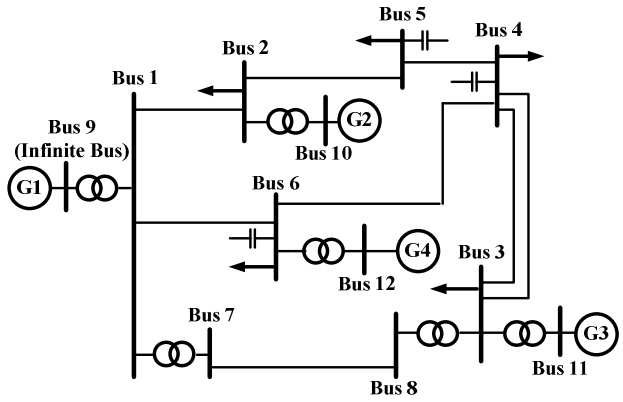

Fig. 6. 12-Bus network used for analysis and simulation of the grid integration of a dish-Stirling solar farm.

Base Case

In the base case, generator 3 (G3) is a conventional thermal power plant, with a synchronous machine generating 200 MW. Simulations indicate that G3 operates in the overexcited mode at a power factor of 0.75 lagging in steady state while maintaining the voltage at bus 11 at 1.01 pu. Operation at such a poor power factor is impractical, and is not typically done in practice. In addition, G3 is not meeting the grid interconnection requirement regarding power factor. The reason for the poor power factor is the load connected at bus 3, which is rated for 320 MW + j240 MVAr, which exceeds the rating of G3. Therefore, significant current must be drawn from connecting lines to supply this load, which requires the automatic voltage regulator of G3 to supply the reactive power to make up for the voltage drop across connecting lines. In order to bring the power factor of the synchronous generator closer to unity, a capacitor bank can be inserted at bus 3 with a MVAr rating determined by

$$Q = P\tan\theta = 200\tan\left(\cos^{-1}(0.75)\right) = 176 \quad MVAr \qquad (4)$$

Simulation results indicate that with the capacitor bank of 176 MVAr in place, the synchronous machine's power factor is approximately unity in steady state, and the voltage at bus 11 is constant at 1.01 pu.

Solar Farm in 12-Bus Network

No Compensation

Before incorporating the solar farm into the 12-bus network, the thermal generator (G3) is removed. With no source connected to bus 11 or reactive power support at bus 3, the voltage at bus 3 drops to 0.78 pu. Adding a 200 MW rated solar farm, (which consists of 8,000 25 kW dish-Stirling units operating at an irradiance of 1000 W/m^2) to bus 11, reduces the voltage at bus 3 even further. However, the voltage at the PCC for a possible solar farm location would not realistically be at 0.78 pu, but adding a capacitor bank rated at 360 MVAr at bus 3 increases the voltage to 1 pu.

Fixed Compensation

Hence a 200 MW rated solar farm is incorporated at bus 11 with a 360 MVAr capacitor connected to bus 3 as shown in Fig. 7. No variable source of reactive power compensation is included. Simulation results for the voltage at the PCC as a function of irradiance appears in Fig. 8. At high irradiance levels, the solar farm is producing near rated power, thus less current is drawn from other system busses. Since less current is drawn, the voltage drop across the connecting lines is less, and thus

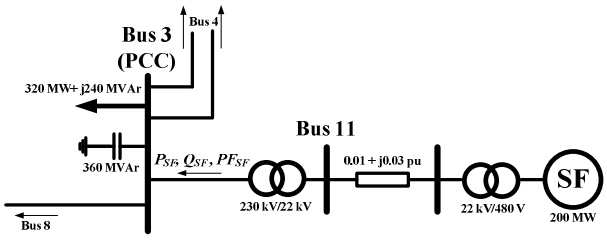

Fig. 7. Connection diagram using only fixed compensation for voltage support in the integration of the solar farm at bus 11.

the 360 MVAr capacitor bank supplies more reactive power than needed, causing the voltage to rise to approximately 1.05 pu. However, at low irradiance, the power factor of the solar farm PF_{SF} follows that shown in Fig. 5(a), causing the voltage at the PCC (V_3) to drop since more current must be drawn from other busses to supply the load, in addition to the reactive power load of the solar farm.

The results of Fig. 8 illustrate the necessity of having variable reactive power compensation since the voltage V_3 changes with irradiance. Further, in more realistic systems, the loads will also vary throughout the day,

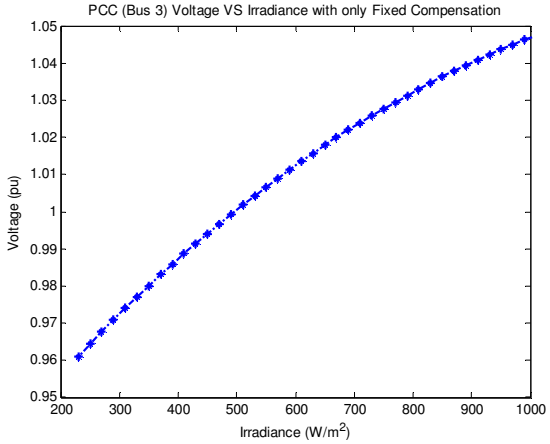

Fig. 8. Bus 3 voltage versus solar irradiance with only fixed compensation.

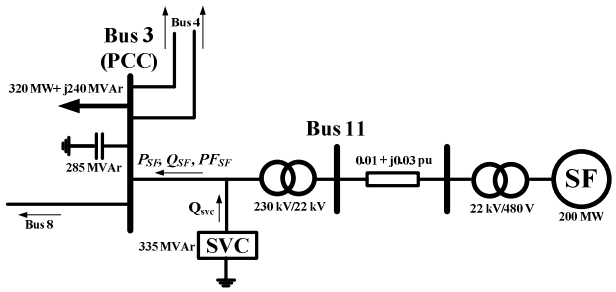

Fig. 9. Connection of solar farm to bus 11 with an SVC used as variable reactive power compensation.

which likely makes fixed compensation inadequate for maintaining the PCC voltage V_3 between 0.95 and 1.05 pu.

Variable Compensation

The solar farm is connected to bus 11 and an SVC is connected at the PCC as shown in Fig. 9. The SVC is rated for 335 MVAr, where the rating is chosen intentionally to be over-sized to ensure the amount of reactive power required to meet the above GIR is achievable. In addition, a fixed capacitor bank of 285 MVAr is connected to bus 3. The fixed capacitor bank is not included as part of the solar farm reactive power compensation since it is included simply to bring the voltage at the PCC above 0.95 pu. In practice, the sizing of fixed compensation and the SVC would be carefully considered in order to minimize the cost of the combined installation. However, for the purposes of this paper, the results are simply intended to demonstrate the behavior of the solar farm power factor PF_{SF} and the PCC voltage V_3 assuming the necessary reactive power compensation is available.

The plot of Fig. 10(a) shows the power factor PF_{SF} of the solar farm over a range of SVC voltage set-points and irradiance levels. The results are obtained by setting the SVC to control the PCC voltage V_3 to a given level over the specified range of irradiance, supplying whatever quantity of reactive power is needed to maintain the commanded voltage level, which is defined in discrete steps over the range shown in Fig. 10(a). The results in Fig. 10(a) show that if the SVC is set to control voltage V_3, the power factor PF_{SF} moves outside the acceptable 0.95 lagging to 0.95 leading range for much of the irradiance and voltage range. The power factor is particularly poor in the region of low irradiance and SVC voltage set point near 1.05 pu. The power factor surface shown in Fig. 10(a) includes both leading and lagging power factors, but does not indicate the power factor orientation (leading or lagging) at a given voltage and irradiance point on the plot. The plot is designed to illustrate the effects of varying irradiance and voltage set points on the power factor *magnitude*, since the GIR specify that the power factor magnitude must be greater than 0.95, regardless of orientation.

The plot of Fig. 10(b) shows the voltage at the PCC with the SVC shown in Fig. 9 set to control the solar farm power factor PF_{SF}. In other words, the SVC injects the amount of reactive power required to reach a power factor set point. The results of 10(b) are shown for a range of solar irradiance levels and a range of solar farm power factor set points between 0.95 leading and 0.95 lagging. The voltage V_3 remains within the acceptable region over most of the irradiance and PF_{SF} levels, accept for high irradiance levels and PF_{SF} values close to 0.95 lagging. At high irradiance levels, the solar farm absorbs most of the reactive power, as shown in Fig. 5(a). Therefore, the SVC is required to supply the reactive power absorbed by solar farm plus the additional amount required to bring its

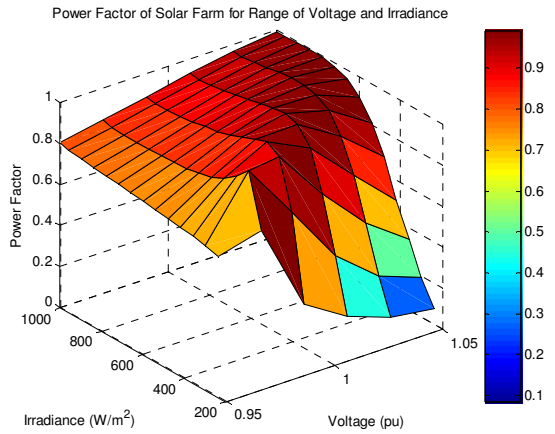

(a)

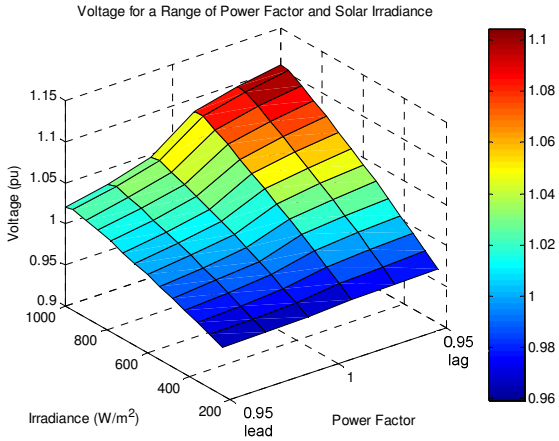

(b)

Fig. 10. (a) Power factor PF_{SF} of the solar farm over a range of irradiance and voltage, with the SVC set to control voltage and (b) voltage at the PCC (bus 3) over a range of solar farm power factor and irradiance.

power factor PF_{SF} to 0.95 lagging. The excess reactive power causes the voltage to rise above 1.1 pu.

Variable Compensation with G3 AVR

The final scenario for interconnection of a solar farm into the 12-bus network is shown in Fig. 11. A 120 MW solar farm is connected to bus 3 of the network *in addition* to the base case 200 MW G3 plant at bus 11. The solar farm power rating is selected so that with an irradiance of 1000 W/m^2, the combination of G3 and the solar farm can meet the real power requirements of the 320 MW local load at bus 3. In this case, the G3 AVR is used to control the voltage at the PCC, while the 335 MVAr SVC controls the power factor of the solar farm. In addition, a 176 MVAr fixed capacitor bank is included at bus 3 to bring the power factor of G3 to unity in the absence of the solar farm, such as the case when the system would be operating during the night, when no irradiance were available. A problem that can arise in using the synchronous generator's AVR to control the voltage of both its own terminals and that of the solar farm is that the power factor of the synchronous generator could potentially move out of an acceptable range in order to maintain the voltage set point at bus 11. Simulation results of the power factor of G3 (bus 11) for varying solar farm power factor and solar irradiance are shown in Fig. 12. The results indicate that G3's power factor stays relatively close to unity over the entire range of solar farm power factors and input solar irradiance, while maintaining the voltage at bus 3 at approximately 1 pu over the entire range.

Simulation results for the SVC reactive power, real and reactive power of the solar farm, and bus 3 voltage are shown in Figs. 13(b), 13(c), and 13(d) for the input irradiance of Fig. 13(a), where it is assumed that the irradiance is uniform over the entire solar farm area. The SVC is set to control the power factor PF_{SF} of the solar

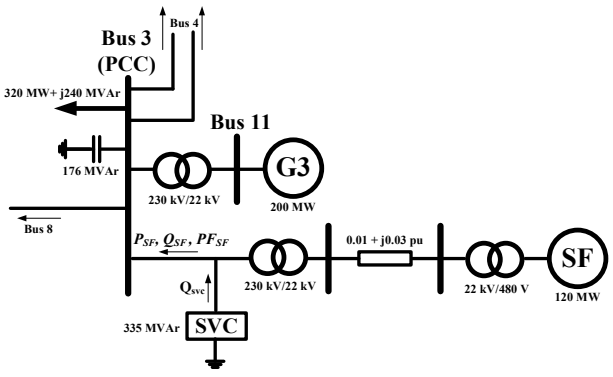

Fig. 11. Interconnection of solar farm to bus 3 in addition to G3, with G3's AVR controlling the bus 3 voltage and the SVC controlling the solar farm power factor.

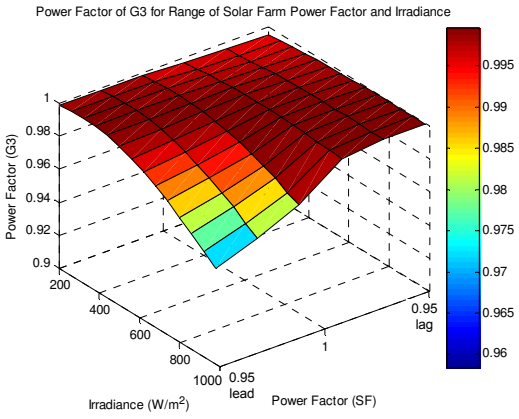

Fig. 12. Power factor of G3 for a range of irradiance and solar farm power factor.

farm to unity. As expected, the real power delivered by the solar farm follows the input irradiance. The reactive power of the solar farm is approximately zero during the cloud transient since the SVC is controlling the power factor PF_{SF} to be unity. Thus, all the reactive power generated by the SVC is supplying the induction generator's reactive power needs. The voltage at bus 3 deviates only slightly from 1 pu, indicating that the synchronous machine's AVR is capable of controlling the bus 3 voltage with the solar farm also connected to bus 3.

Conclusion

With no synchronous generator connected to bus 11, bus 3 can be considered a "weak" grid PCC. Therefore, adding a solar farm to a weak grid may not always be possible, since the results show that the power factor and voltage requirements cannot both be met over all irradiance levels in the case with a 200 MW solar farm incorporated at bus 11. However, because the voltage can be brought to 1 pu with fixed capacitors at bus 3 with no power source connected to bus 11 (or bus 3), the solar farm could be reduced in MW rating, which would decrease its impact on the voltage at bus 3 over varying irradiance levels and solar farm power factor. Therefore, in addition to varying irradiance levels due to cloud cover, the power rating of the solar farm also plays an important part in determining whether the solar farm can meet GIR.

When the solar farm is integrated into the 12-bus network near a synchronous generator, the PCC closely resembles a "strong" grid. In this scenario, the results with both G3 and the solar farm demonstrate that the solar farm can operate well within the power factor requirements, while G3 can maintain a suitable power factor and control the PCC voltage. Therefore, the MW rating of the solar farm could potentially be increased, and the system would still be capable of meeting the GIR.

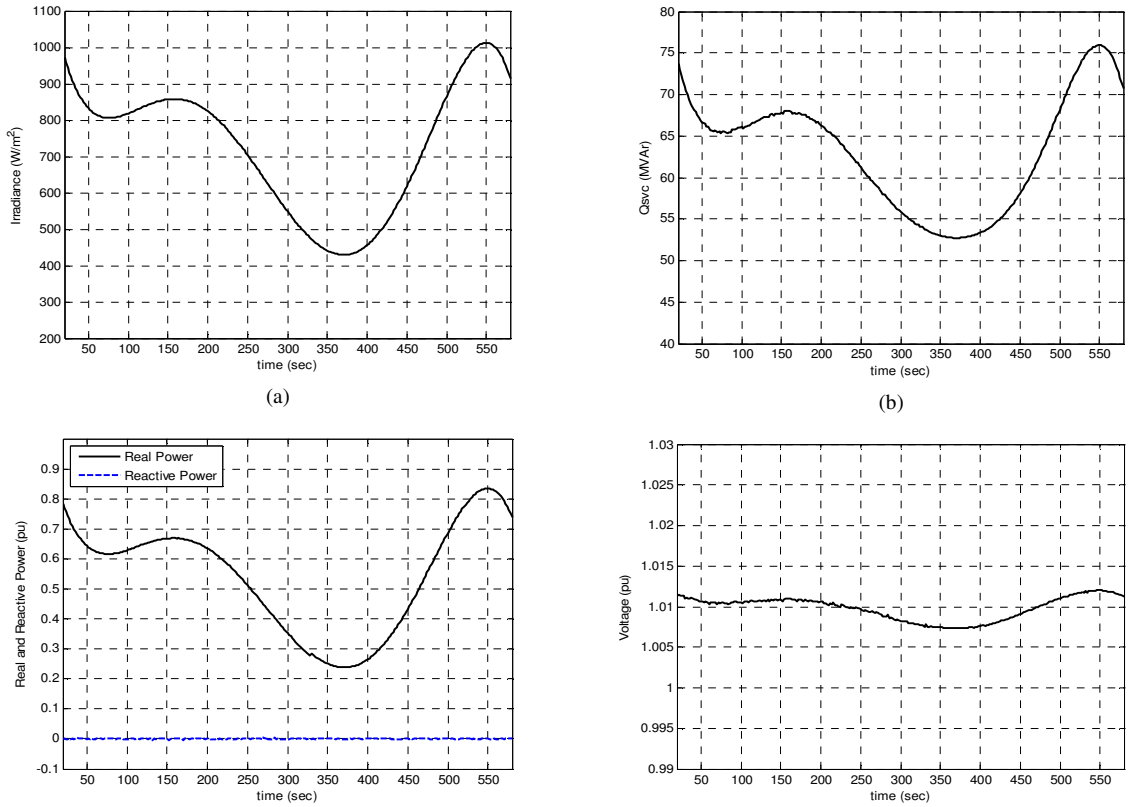

Fig. 13. Simulation results of the solar farm (b) SVC reactive power output, (c) real and reactive power, and (d) PCC (bus 3) voltage for a cloud transient using the input irradiance waveform of (a).

Simulation results for the various scenarios discussed above for integrating a solar farm into the 12-bus network illustrate the need for significant reactive power compensation in order to meet both voltage and power factor GIR. While the variable reactive power compensation discussed in this paper has been over-sized to ensure that the solar farm could meet the grid interconnection requirements over all irradiance levels, in practice the variable reactive power compensation rating would have to be minimized in order to reduce cost. In addition, the effects of time-varying loads and grid connection requirements involving low voltage ride-through will significantly affect the sizing of the reactive power compensation.

References

[1] Stirling Energy Systems. (2008, Feb.). "Sandia, Stirling Energy Systems set new world record for solar-to-grid conversion efficiency," Press Release [Online]. Available: http://www.stirlingenergy.com/pdf/2008-02-12.pdf

[2] Tessera Solar. (2010, Jan.). "Tessera Solar and Stirling Energy Systems Unveil World's First Commercial Scale Suncatcher™ Plant, Maricopa Solar, with Utility Partner Salt River Project," Press Release [Online]. Available: http://tesserasolar.com/north-america/pdf/2010_01_22.pdf

[3] Y. Zhang and B. Osborn, "Solar Dish-Stirling Power Plants and Related Grid Interconnection Issues," in *Proc. 2007 IEEE PES General Meeting*, Jun. 24-28, 2007, Tampa, FL.

[4] T. Mancini, P. Heller, B. Butler, et. al, "Dish-Stirling Systems: An Overview of Development and Status," in *Journal of Solar Energy Engineering*, vol. 125, pp. 135-151, May 2003.

[5] D. Howard and R. G. Harley, "Modeling of Dish-Stirling Solar Thermal Power Generation," in *Proc. 2010 IEEE PES General Meeting*, Jul. 25-29, 2010, Minn., MN. [Accepted].

[6] D. Howard, J. Liang, and R.G. Harley, "Control of Shaft Speed and Receiver Temperature in Dish-Stirling Solar Power Generation for Power Grid Integration," in *Proc. 2010 IEEE Energy Conversion Congress & Expo*, Sept. 12-16, 2010, Atlanta, GA. [Accepted].

[7] USA Federal Energy Regulatory Commission, "Interconnection for Wind Energy," 18 CFR Part 35, Docket No. RM05-4-000 – Order No. 661, June, 2005.

[8] C.W. Lopez and K.W. Stone, "Performance of the Southern California Edison Company Stirling Dish," Sandia National Laboratories, Albuquerque, NM, DOE Contract DE-AC04-94AL85000, Oct. 1993.

[9] S. Jiang, U.D. Annakkage, and A.M. Gole, "A Platform for Validation of FACTS Models," in *IEEE Transactions on Power Delivery*, Vol. 21, No. 1, Jan. 2006.